

Morphology and Microstructure in Electrochemical Deposition of Zinc

D. Grier, E. Ben-Jacob, Roy Clarke, and L. M. Sander

Department of Physics, The University of Michigan, Ann Arbor, Michigan 48109

(Received 21 October 1985)

We report an experiment in the Ohmically-limited electrochemical deposition of zinc which explicitly probes the link between microscopic structure and macroscopic morphology in the development of interfacial patterns far from equilibrium. We report a previously unrecognized transition region between diffusion-limited aggregation and dendritic growth; analysis of the microstructure suggests mechanisms for the macroscopic expression of crystalline anisotropy. We also report the discovery of a metastable crystalline form of zinc produced during electrodeposition.

PACS numbers: 61.50.Cj, 05.40.+j, 61.90.+d

When a nonequilibrium system grows by the addition of material by diffusion a very rich variety of macroscopic shapes are possible. The best known cases occur when diffusion-limited solidification gives rise to well-defined patterns. Most common are dendritic (that is, branched) and needlelike crystal shapes which reflect the underlying symmetry of the crystal lattice. However, very similar processes such as diffusion-limited aggregation¹ (DLA) are known to give rise to disorderly fractals with no apparent symmetry except for dilation. It is extremely interesting to try to understand the conditions under which these two types of growth occur. This paper reports a contribution to that task.

An essential step in understanding the situation was taken when studies of models of crystallization^{2,3} indicated a well-defined crossover from stable growth of a tip of the solid (possibly leaving side branches behind) to unstable tip splitting as crystal anisotropy decreases. A study of a fluid-flow system⁴ and further theoretical work⁵ again identified two regimes of growth depending on anisotropy and showed that the tip-splitting regime is the same as fractal growth in certain cases. Recent computer simulation studies of DLA-like growth models have shown analogous effects.⁶⁻⁹

Electrodeposition offers a very attractive way to study these phenomena in an experiment on real crystals. Brady and Ball¹⁰ showed how to make three-dimensional copper deposits that were DLA-type fractals and had no apparent symmetry. Matsushita *et al.*¹¹ produced similar two-dimensional fractal zinc deposits. On the other hand, dendritic shapes with evident crystal anisotropy effects are well known¹² in electrochemistry. We report here an experiment in which we have observed, for the first time, the crossover between the two types of crystal formation by electrochemical deposition of zinc. (Zinc is a better candidate than copper in this regard because its hcp structure has more intrinsic anisotropy than cubic copper. In fact, we tried, and failed, to observe the crossover in copper; this indicates, once more, the critical role of small differences in crystal anisotropy.)

Our electrodeposition cell consists of a copper ring anode 12.7 cm in diameter set into a piece of Plexiglas with 0.1 mm exposed above the surface. Aqueous zinc sulfate solution, pH 7, is poured into this reservoir and is confined in a uniform 0.1-mm film by the addition of an upper plate. The cathode and growth site is a fine copper wire introduced through a hole in the lower plate centered within the ring. When a voltage is applied across the cell, zinc ions migrate to the central wire where they accrete. An inert field wire 0.25 mm from the inner edge of the anode was used to make the cell a potentiostat. We find that the cell is Ohmic both by measuring the I - V characteristics and also by measuring the response to a small-amplitude ripple imposed on the dc current.

In Figs. 1 and 2 we show that by varying the concentration of electrolyte and cell voltage we do indeed produce a wide variety of patterns of deposits, some quite disorderly, and some of which are ordinary dendrites. In the remainder of this paper we will try to understand these patterns.

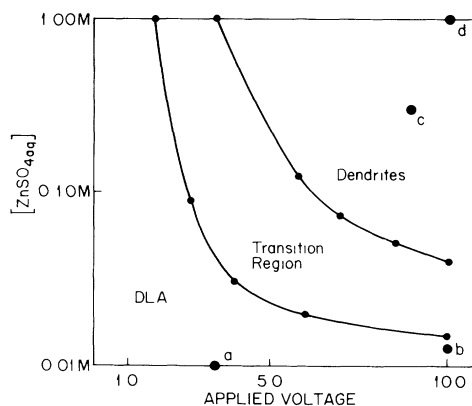


FIG. 1. Observed regions of pattern formation in electrochemical deposition. Solid lines separate regimes where distinct morphologies could be identified. The indicated data points are accurate to $\pm 0.01M$ and $\pm 0.02V$. Points labeled a - d correspond to the photographs in Fig. 2. The data are a summary of about 250 growth conditions.

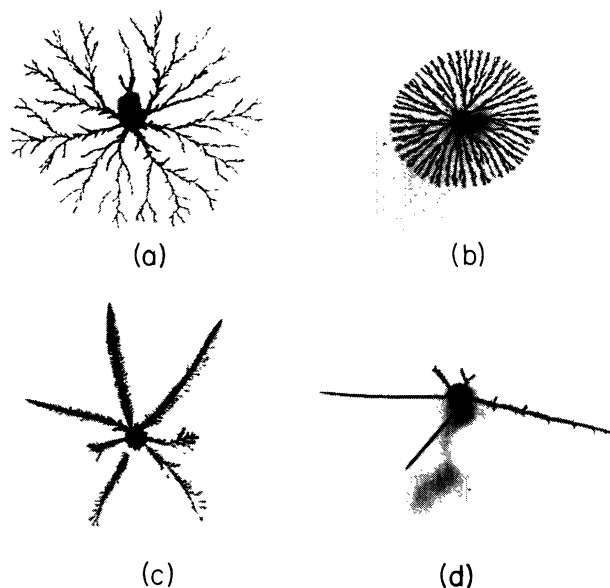


FIG. 2. Patterns in electrochemical deposition of zinc. Deposits (a)–(d) were grown under conditions indicated by points *a*–*d* in Fig. 1, respectively. (a) DLA, (b) dense radial, (c) dendritic; and (d) needle crystal in the extreme dendritic limit.

We first note that the rate-limiting step in our cell (and also in Ref. 11, we think) is not ion diffusion as it was in Ref. 10. This is clear for two reasons: The patterns that we observe show structure on scales much larger than any diffusion length in the system. Also, the cell is Ohmic. If concentration gradients actually were significant in the cell then the negative ions which play no role in the chemistry would eventually screen the field and eliminate conduction current flow. We think that this does not happen because natural convection in the cell stirs the electrolyte on scales larger than the double layer which would form. We have directly observed the presence of this rapid stirring by adding a dye to track fluid motion. As we would expect in a cell 0.1 mm thick, the convection takes place on a small scale (< 0.05 mm) and cannot account for the patterns that we see. The detailed mechanism is not clear.

Even though the dominant current in our system is a conduction current we expect the phenomenology outlined above for the diffusion-limited system to apply. This is because¹⁰ for steady-state current flow we have equations describing the growth that are of an identical form as in the diffusion-limited case. We have the same growth instabilities (i.e., largest growth at tips); these give rise to the patterns that interest us.

We can use the following simple ideas to interpret our observations. The total current that feeds the growth is, for our geometry and the assumption of

small-scale random stirring,

$$I(t) = \frac{2\pi\sigma Vs}{\ln(R/a)}, \quad (1)$$

where V is the voltage, σ the conductivity, R the radius of the outer electrode, $a(t)$ an average radius of the deposit, and s the depth of the electrolyte. Thus the overall rate of growth has as control parameter (for fixed deposit size) σVs , i.e., for dilute electrolyte, nVs , where n is the Zn^{++} concentration in solution.

The essential physics that we are investigating here is the way in which microscopic anisotropy is expressed in macroscopic shapes. It was found in previous works^{2,3} that a useful way to represent this connection is in terms of the boundary condition which represents a different rate of sticking on various crystal surfaces. Since the difference in growth rate in different directions is proportional to the total growth, i.e., to the incoming current, we expect anisotropy to have larger effects (and give rise to dendrite and needle crystals) at larger control parameters, e.g., at larger voltage. This expectation is satisfied in the experiment of Ref. 4, where larger pressure enhances anisotropy effects.

The results of a survey of the macroscopic morphology of the deposits are summarized in Fig. 1, which we classify into two kinds of pattern: disorder fractal growth at low driving force, where growing tips often split, and stable dendritic growth at high driving force. Between these regimes there is a regime of crossover (labeled “transition region” in Fig. 1). Differentiation among the growth regimes was based on comparison with the results of computer models, the fractal dimension of the deposits, and details of microstructure which will be discussed below. We measured fractal dimensions by digitizing photographs and taking the best-fit slope of $\log[N(r)]$ vs $\log(r)$, where $N(r)$ is the number of pixels contained within a radius r . The scan resolution is 256×256 pixels and our program was calibrated with use of objects of known fractal dimension in random orientations.

Fine highly branched structures such as that in Fig. 2(a) were included among the fractals, as were small nonfractal dense aggregates which seemed to be undergoing tip splitting, but were round in overall shape [Fig. 2(b)]. We measured a fractal dimension of $D = 1.75 \pm 0.03$ over most of the highly branched regime in reasonable agreement with computer simulations. Approaching the transition region, however, we observed an increase in fractal dimension with increasing voltage and increasing concentration similar to the trend reported by Matshushita *et al.*¹¹

Dendritic morphology is shown in Fig. 2(c). The extreme limit of dendritic growth of our system appears to be very stable straight needlelike deposits such as Fig. 2(d), whose fractal dimension approaches

1. This is in contrast with the experiment of Ref. 4 in which dendrites become needlelike upon crossover from tip splitting and then become more highly decorated with increasing driving force. The difference suggests that the anisotropy in the case of electrochemical deposition is introduced through different boundary conditions.¹³ We have been rather conservative in classifying patterns into the transition region. Included in this regime are deposits that are inhomogeneous in the sense that they show bursts of dendritic growth alternating with tip splitting. These probably arise from inhomogeneities in our cell. Within these broad (and somewhat subjective) limits the expectation that $nV = \text{const}$ should demarcate regimes of growth is obeyed. In principle, since the growth regimes represent a change in symmetry, the boundaries should be sharp in ideal conditions, and there is probably no separate transition regime.

In order further to elucidate the crossover we have examined the microstructure of the deposits with electron microscopy and x-ray diffraction. Material from the deposits is transparent to 75-keV electrons, indicating that they are typically on the order of 200 Å thick. Transmission electron micrographs of the deposits suggest that the structural differences between the modes of growth persist down to the smallest length scales. It is unlikely that convective stirring can operate on the scale of the micrograph. On these scales, the structure is controlled by particle diffusion.

Undamaged material from DLA-like aggregates is shown in Fig. 3(a), displaying tips which are rough and unafaceted down to a scale less than 300 Å. Selected-area electron diffraction patterns from these regions [see inset of Fig. 3(a)] suggest that there is no long-range ordering in DLA-like aggregates. The microscopic structure appears to have intermediate-range order with correlation lengths of typically ~ 50 Å. The isotropic rings indicate a lack of orientational order within the selected area of roughly 1 μm .

Dendritic tips, such as the one shown in Fig. 3(b), are characterized by large, rounded crystal facets and areas of smoothly curved features. Diffraction patterns both from the facets and also from several series of ripples believed to be side branches (not shown) reveal sharply defined diffraction peaks and indicate long-range crystalline order. Furthermore, undamaged dendritic tips uniformly produce diffraction patterns with the c axis of hcp zinc perpendicular to the plane of deposition. No such correlation is evident in DLA-like material. This strongly supports the assertion that the stacked-plane structure of hcp zinc is the microscopic source of the anisotropy which stabilizes dendritic growth in zinc.

Additional diffraction peaks obtained at low beam current indicate a superlattice modulation of zinc in the planes normal to the c axis. This structure anneals

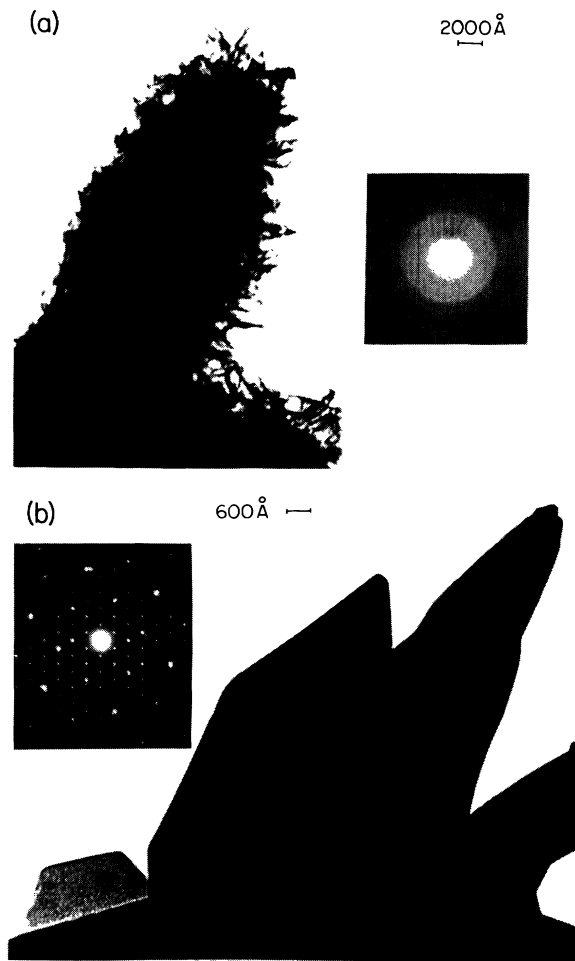


FIG. 3. Transmission electron micrographs of electro-deposited zinc. (a) DLA-growth tip; inset: electron diffraction pattern of tip showing diffuse rings. (b) Dendritic sample; inset: superlattice diffraction pattern from grain in lower left of micrograph. The more intense spots correspond to the $(hk0)$ pattern of bulk zinc.

to the usual hcp conformation and the additional spots disappear under intense electron-beam illumination. This modulation also appears as additional Bragg peaks in the x-ray diffraction of all samples albeit very diffuse in the DLA regime, indicating that the relevant parameter in the microscopic structural transition in our system is the appearance of long-range order in the dendritic regime. This observation supports the assumption that anisotropy stabilizes pattern through a kinetic term. The additional Bragg peaks also disappear after the material has been allowed to age without oxidation. Details of this crystalline structure will form the subject of a subsequent publication.¹⁴

Energy-dispersive electron-beam analysis shows somewhat less than 0.01M copper impurities. There is

no evidence for hydrolysis of water in our experiments.

In summary, we have demonstrated a crossover from disorderly growth to dendritic morphology. We also show that there is a close relationship between the microstructure and the morphology of growth.

These results suggest that a similar relationship may be operative in other forms of diffusion-limited growth, in particular, directional solidification.¹⁵

We acknowledge useful discussions with R. Ball, K. Mullen, J. Gollub,¹⁶ and A. Kapitulnik. Sarah Wilson helped with some of the experiments. The research was supported in part by a Rackham Award (E.B.-J.), by the National Science Foundation through Grants No. DMR8404975 (R.C.) and No. DMR-8505474 (L.M.S.), and U.S. Army Research Office Grant No. DAAG-29-83-K-0131.

¹T. A. Witten, Jr., and L. M. Sander, Phys. Rev. Lett. **47**, 1400 (1981), and Phys. Rev. B **29**, 5686 (1983).

²E. Ben-Jacob, N. D. Goldenfeld, B. G. Kotliar, and J. S. Langer, Phys. Rev. Lett. **53**, 2110 (1984); E. Ben-Jacob, N. D. Goldenfeld, J. S. Langer, and G. Schön, Phys. Rev. Lett. **51**, 1930 (1983), and Phys. Rev. A **29**, 330 (1984).

³D. Kessler, J. Koplik, and H. Levine, Phys. Rev. A **32**, 1930 (1985), and **30**, 3161 (1984); R. Brower, D. Kessler, J. Koplik, and H. Levine, Phys. Rev. Lett. **51**, 1111 (1983), and Phys. Rev. A **29**, 1335 (1984).

⁴E. Ben-Jacob, R. Godbey, N. Goldenfeld, J. Koplik,

H. Levine, T. Mueller, and L. M. Sander, Phys. Rev. Lett. **55**, 1315 (1985).

⁵L. M. Sander, P. Ramanlal, and E. Ben-Jacob, Phys. Rev. A **32**, 3160 (1985).

⁶T. Vicsek, Phys. Rev. Lett. **53**, 2281 (1984).

⁷F. Family, T. Vicsek, and P. Meakin, Phys. Rev. Lett. **55**, 641 (1985).

⁸M. Kolb, to be published.

⁹P. Garik, Phys. Rev. A **32**, 3156 (1985).

¹⁰R. Brady and R. C. Ball, Nature (London) **309**, 225 (1984).

¹¹M. Matsushita, M. Sano, Y. Hayakawa, H. Honjo, and Y. Sawada, Phys. Rev. Lett. **53**, 286 (1984).

¹²For a review of the theory of electrocrystallization, see René Winand, Trans. Inst. Min. Metall., Sect. C **84**, 67 (1975).

¹³P. Garik, K. Mullen, D. Grier, and E. Ben-Jacob, unpublished.

¹⁴R. Clarke, D. Grier, E. Ben-Jacob, and L. M. Sander, unpublished.

¹⁵A. Libchaber, private communication.

¹⁶An experiment very similar to ours was simultaneously performed by Y. Sawada, A. Dougherty, and J. P. Gollub, preceding Letter [Phys. Rev. Lett. **56**, 1260 (1986)]. Their observations and conclusions are also quite similar to ours, the main difference being in the interpretation of deposits which have many tip splittings, but which are round in overall shape and not fractal. These patterns (which we have lumped with the fractals) are very puzzling from the theoretical point of view, and indicate that the speculation of Ref. 4 that tip splitting is a sufficient condition for the forming of diffusion-limited aggregates may not be correct. It is certainly a necessary condition. Further work on these intriguing "dense radial" patterns is in progress.

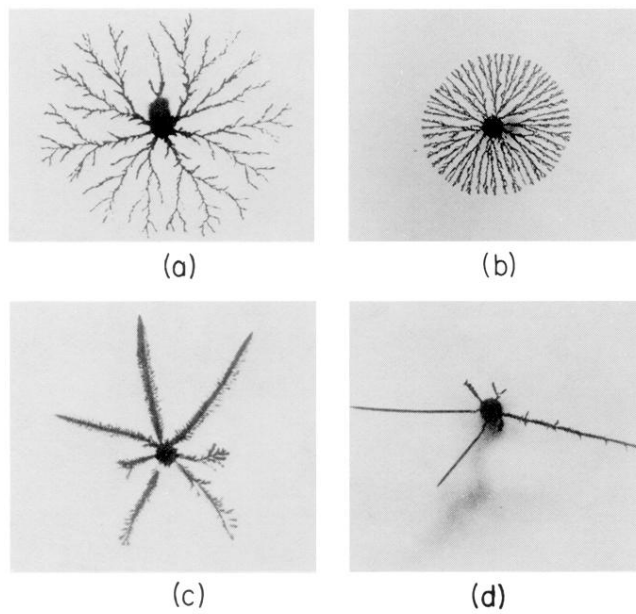


FIG. 2. Patterns in electrochemical deposition of zinc. Deposits (a)–(d) were grown under conditions indicated by points *a*–*d* in Fig. 1, respectively. (a) DLA, (b) dense radial, (c) dendritic; and (d) needle crystal in the extreme dendritic limit.

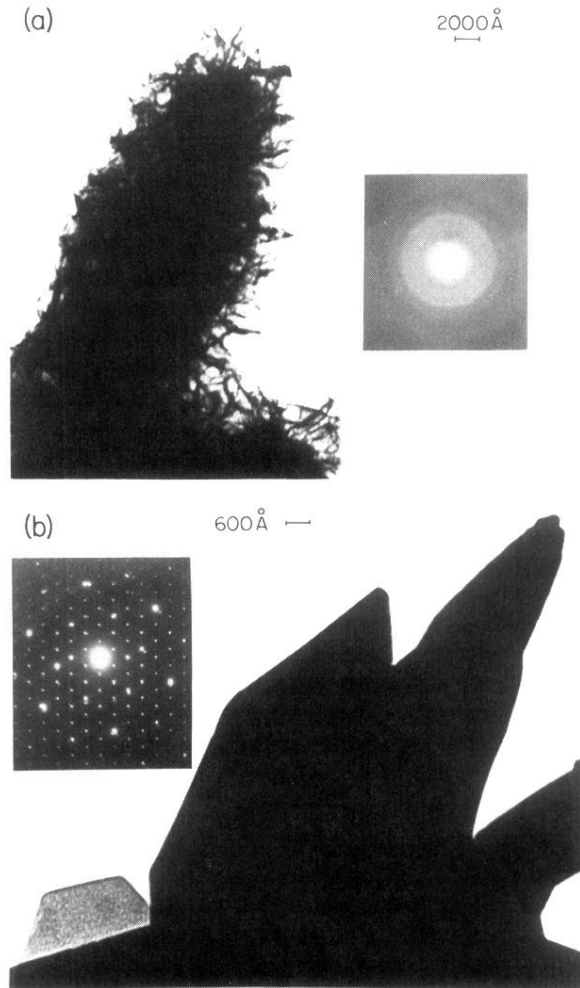


FIG. 3. Transmission electron micrographs of electro-deposited zinc. (a) DLA-growth tip; inset: electron diffraction pattern of tip showing diffuse rings. (b) Dendritic sample; inset: superlattice diffraction pattern from grain in lower left of micrograph. The more intense spots correspond to the $(hk0)$ pattern of bulk zinc.